Thermomechanical Two-Mode Squeezing in an Ultrahigh-Q Membrane Resonator

Y. S. Patil, S. Chakram, L. Chang, and M. Vengalattore

Phys. Rev. Lett. **115**, 017202 — Published 29 June 2015

DOI: 10.1103/PhysRevLett.115.017202

Thermomechanical two-mode squeezing in an ultrahigh Q membrane resonator

Y. S. Patil, S. Chakram, L. Chang and M. Vengalattore
Laboratory of Atomic and Solid State Physics, Cornell University, Ithaca, NY 14853

We realize a quantum-compatible multimode interaction in an ultrahigh Q mechanical resonator via a reservoir-mediated parametric coupling. We use this interaction to demonstrate nondegenerate parametric amplification and thermomechanical noise squeezing, finding excellent agreement with a theoretical model of this interaction over a large dynamic range. This realization of strong multimode nonlinearities in a mechanical platform compatible with quantum-limited optical detection and cooling makes this a powerful system for nonlinear approaches to quantum metrology, transduction between optical and phononic fields and the quantum manipulation of phononic degrees of freedom.

PACS numbers: 85.85.+j,42.50.-p,62.25.-j,42.50.Dv

The control, measurement and manipulation of mesoscopic mechanical resonators by coherent optical fields has garnered widespread attention in recent years for potential applications to quantum metrology as well as to foundational studies of the quantum-to-classical transition and the quantum mechanics of macroscopic objects [1–4]. Notable accomplishments in recent years include the optical cooling of mechanical modes to the quantum regime [5, 6] and the detection of mechanical motion with an imprecision below the standard quantum limit [7, 8].

Building upon these developments, attention has now been directed towards the creation of nonclassical mechanical states and the manipulation of phononic fields in a manner akin to quantum optics in nonlinear media. In contrast to the cooling and detection of mechanical motion, the creation of nonclassical states requires strong nonlinear interactions involving the mechanical degree of freedom. Accordingly, several studies have been devoted to the realization of such interactions through parametric processes [9–13], optically mediated nonlinearities [14], dispersive coupling to an auxiliary quantum system [15, 16], backaction-evading measurements [17, 18] and active feedback [19–22]. Notwithstanding the diversity of such schemes, it has remained a significant challenge to juxtapose strong, tunable and quantum-compatible nonlinear interactions with the stringent constraints for ground state cooling and quantum control of a mechanical resonator.

Here, we demonstrate that strong mechanical nonlinearities can co-exist with low dissipation by exploiting the concept of reservoir engineering [23–26] - the control of interactions within a system by appropriate design of its environment. While most proposals along these lines have centered on mechanical control by tuning the properties of an optical reservoir, we show that reservoir engineering can be effected through purely mechanical means. This opens the concomitant prospect of realizing a wide range of novel interactions in micro- and nanomechanical systems through appropriate geometric and material design. In our work, a strong nonlinear interaction between distinct modes of a membrane resonator is realized by the parametric mediation of a substrate excitation. We use this nonlinearity to demonstrate nondegenerate parametric amplification and thermomechanical noise squeezing, finding excellent agreement with a theoretical model of this nonlinear interaction over a large dynamic range. The combination of strong multimode mechanical nonlinearities, optical addressability of individual mechanical modes, large $f \times Q$ products [27], compatibility with optomechanical cooling to the quantum regime [28, 29] and quantum-limited optical measurement makes this a powerful system for quantum-enhanced metrology and the quantum manipulation of phononic fields.

The mechanical resonators in our study are LPCVD silicon nitride (SiN) membrane resonators manufactured by NORCADA Inc. The membranes are deposited on single crystal silicon wafers and have typical lateral dimensions of 5 mm. In previous work [27], we have identified the role of the substrate in inducing the hybridization of proximal eigenmodes and in modifying the dissipation of the resultant hybridized modes. This leads to the robust formation of a large number of mechanical modes with quality factors $Q \sim 50 \times 10^6$ and $f \times Q \sim 1 \times 10^{14}$ Hz.

In addition to modifying the modal geometry and dissipative properties, the substrate can also mediate and enhance nonlinear interactions between distinct eigenmodes of the resonator. This is especially significant for parametric processes that involve the interaction of two membrane modes mediated by a discrete excitation of the substrate, since the coupling strength is now enhanced by the quality factor of the relevant substrate mode. In our work, this nonlinear interaction between mechanical modes at frequencies ω_i, ω_j is induced by parametrically actuating the substrate at frequencies near $\omega_i + \omega_j$, either by a piezo-electric voltage or a photothermal modulation.

A schematic of the experimental system is shown in Fig. 1. The mechanical motion of the membrane is optically detected in a Michelson interferometer with a displacement sensitivity of 0.03 pm/Hz$^{1/2}$ for typical powers of 200 μW incident on the membrane. Distinct eigenmodes are resolved through phase sensitive lock-in detection. The membrane modes exhibiting the two-mode nonlinearities studied in this work are characterized by eigenfrequencies $\omega_i/2\pi \approx 1.5$ MHz, quality factors

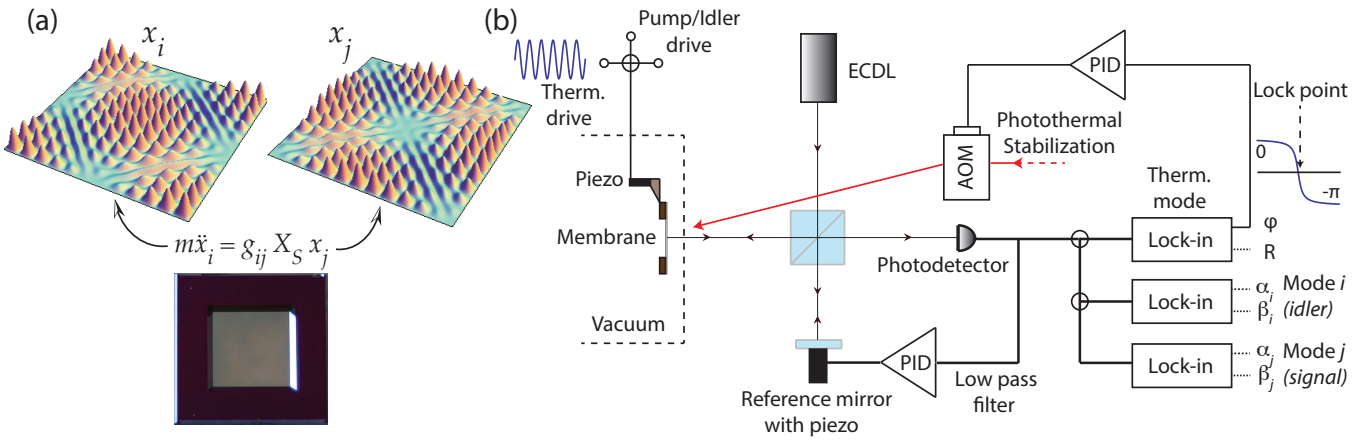

FIG. 1. (a) The resonator consists of a high-stress silicon nitride membrane deposited on a silicon substrate. Distinct eigenmodes of the membrane resonator (representative eigenfunctions shown) with frequencies $\omega_{i,j}$ are coupled via a substrate-mediated interaction. This two-mode interaction can be controlled by actuating the substrate to an amplitude X_S at frequencies close to $\omega_i + \omega_j$. (b) Experimental schematic: Mechanical motion of the membrane is optically detected in a Michelson interferometer, with the two membrane modes (i, j) distinguished by phase-sensitive lock-in detection. The eigenfrequency of a third, high-Q mechanical mode is continuously monitored and acts as a mechanical 'thermometer'. The resonator modes are actively frequency stabilized to this thermometer mode by photothermal feedback. In the presence of this feedback, the frequency stability of each resonator mode is better than 1 ppb over 1000 seconds.

$Q > 10 \times 10^6$, typical mechanical linewidths $\gamma_i/2\pi < 100$ mHz and $|\omega_i - \omega_j| > 10^6\,\gamma_{i,j}$. While the large quality factors are crucial to realizing long coherence times, the narrow linewidths also pose stringent requirements of thermal stability in order to resolve thermomechanical motion and the presence of non-thermal correlations. To achieve the requisite frequency stability, the membrane modes are actively stabilized by photothermal feedback (see Supplementary Information, see also [30]).

The substrate-mediated coupling between a pair of membrane modes can be modeled by an interaction $\mathcal{H}_{ij} = -g_{ij} X_S x_i x_j$ where g_{ij} parametrizes the strength of the two-mode coupling, X_S is the displacement of the substrate (or 'pump') and $x_{i,j}$ denotes the displacement of the two membrane modes. This interaction can be attributed to a parametric excitation of a discrete mode of the substrate at a frequency $\omega_S = \omega_i + \omega_j$, that couples the membrane modes. Actuation of the substrate at this frequency thus leads to nondegenerate parametric amplification of the individual membrane modes.

As is well known in such parametric amplifiers, a sufficiently strong interaction (or a large actuation of the pump field) leads to an instability and self-oscillation of the individual membrane modes. In the case of resonant actuation, our two-mode model predicts a threshold amplitude for self-oscillation given by (see SI),

$$X_{S,th}(g) = 2\sqrt{\frac{1}{g^2} \times \frac{1}{\chi_i \chi_j}} \propto \sqrt{\frac{1}{g^2}\frac{1}{Q_i Q_j}} \qquad (1)$$

where $\chi = (m\omega\gamma)^{-1}$ are the on-resonant mechanical susceptibilities of the two membrane modes and g is the strength of the two-mode coupling. The inverse dependence of the threshold pump amplitude on the quality factors of the high-Q membrane modes leads to strong nonlinear behavior even for pump displacements on the order of 10 fm. Past the instability threshold, we observe amplification of the membrane modes by more than 30 dB (see Fig. 2(a)).

While the parametric amplification of the membrane modes can be regarded as a down-conversion of substrate excitations, a related process is the up-conversion of excitations from the membrane into the substrate. In the absence of substrate motion, actuation of the membrane modes can lead to coherent transfer of energy from the membrane into the substrate. From the perspective of either membrane mode, this parametric transfer of energy into the far lossier substrate results in a dissipation rate that is dependent on the amplitude of the other membrane mode.

To study this process, the mechanical ring-down time τ of a membrane mode j was measured in the presence of a large amplitude actuation of its partner mode i. Care was taken in these measurements to maintain the amplitude of mode j in the linear response regime. The two-mode upconversion process results in an effective quality factor $Q_j(x_i) = \omega_j \tau(x_i)/2$ and an effective mechanical linewidth $\gamma_j(x_i) = 2/\tau(x_i)$ that is in excellent agreement with the prediction of the two-mode model (see SI),

$$\gamma_j(x_i) \approx \frac{\gamma_S}{2}\left[1 + \frac{2\gamma_j}{\gamma_S} - \sqrt{1 - \left(\frac{x_i}{\xi}\right)^2}\right] \qquad (2)$$

where $\gamma_j \ll \gamma_S$ are the intrinsic mechanical linewidths

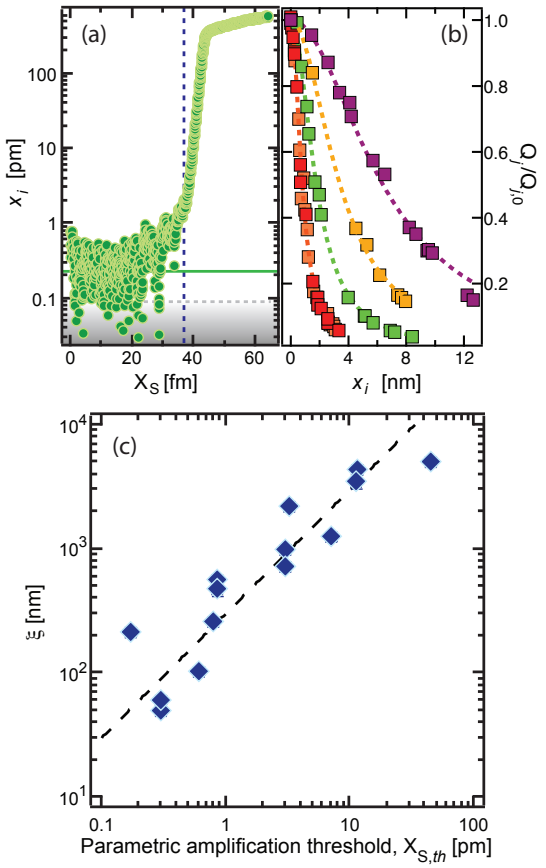

FIG. 2. (a) Parametric amplification of a membrane mode due to actuation of the substrate. The vertical line indicates the threshold for parametric instability. The solid green line indicates the thermomechanical amplitude of the membrane mode. The dashed grey line shows the detection noise floor. (b) In the absence of the parametric drive, large amplitude oscillations of either membrane mode (x_i) results in increased dissipation (and a lower quality factor Q_j) of the other mode due to up-conversion of excitations into the substrate. The variation of the normalized dissipation ($Q_j/Q_{j,0}$), shown above for various pairs of coupled modes, is well described by a characteristic length scale ξ (see text). (c) The linear dependence of the length scale ξ (extracted from data such as shown in (b)) *vs* the threshold amplitude for parametric instability, as predicted by the two-mode model. See SI for details of the various modes depicted above.

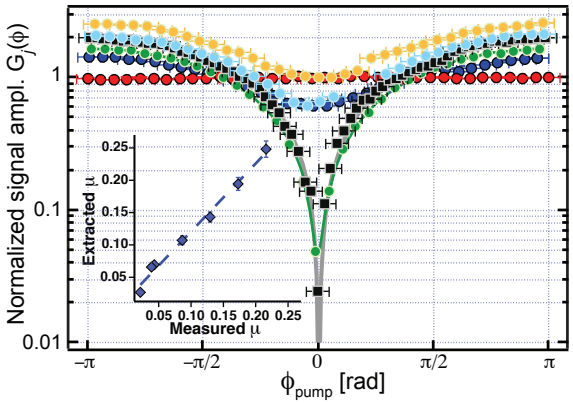

FIG. 3. Phase-sensitive amplification, $G_j(\phi)$, versus the phase of the pump excitation. Data shown correspond to normalized pump amplitudes $\mu = X_S/X_{S,th} = 0, 0.021, 0.038, 0.042, 0.086, 0.13$ (red, blue, green, black, cyan, orange). For these data, the threshold for parametric self-oscillation corresponds to $X_S = 40$ fm, the signal and idler modes are driven to $35 \times (k_B T/m\omega_j^2)^{1/2}$ and $400 \times (k_B T/m\omega_j^2)^{1/2}$ respectively, corresponding to $\eta = 14.4$. Inset: Estimate of the pump amplitude from fits to these data agree with the actual pump amplitude to within 5%.

of membrane mode j and the substrate mode (see Fig. 2(b)). The length scale ξ denotes the characteristic amplitude of mode i when the dissipation rate of the membrane mode j matches that of the substrate, i.e. the maximal rate of up-conversion of energy from the membrane into the substrate. Due to the large mismatch between the intrinsic dissipation rates and masses of the substrate and the membrane, this up-conversion process requires displacements of the membrane modes that are more than five orders of magnitude larger than typical thermomechanical motion (see Fig. 2), and much larger than the typical amplitudes of motion considered in this work.

While seemingly distinct processes observed at vastly differing scales of displacement (fm *vs* nm), nondegenerate parametric amplification and nonlinear dissipation due to up-conversion of excitations into the substrate both owe their origins to the two-mode nonlinearity. Indeed, the model predicts that the length scale ξ that parametrizes two-mode control of mechanical dissipation, can be related to the threshold amplitude $X_{S,th}$ according to the relation $\xi(g) = \frac{1}{2}(\gamma_S/\gamma_i)^{1/2}(\chi_j/\chi_S)^{1/2} \times X_{S,th}(g)$. Given that the quantity $(\gamma_S/\gamma_i)^{1/2}(\chi_j/\chi_S)^{1/2}$ does not vary significantly for the mode pairs studied (see SI), we expect a linear relation between $\xi(g)$ and $X_{S,th}(g)$. Through independent measurements of parametric amplification thresholds and nonlinear two-mode dissipation for a wide range of membrane mode pairs, we have verified this linear dependence (see Fig. 2(c)). As can be seen, the various mode pairs that were studied exhibit interaction strengths that vary over three orders of magnitude. The close agreement between our measurements and the predictions of the model over a large dynamic range of parameters further affirms the robustness and fidelity of this nonlinear interaction in our system.

Having established the accuracy of our two-mode model, we now discuss the dynamics of this nondegenerate parametric amplifier for a pump field driven below the threshold $X_{S,th}$. In this regime, weak actuation of a membrane mode i (idler mode) results in the phase coherent production of down-converted phonons in the other membrane mode j (signal mode). This down-converted

field, which has a well determined phase relationship with the pump and idler fields, can coherently interfere with any pre-existing signal field. Thus, the amplitude of the signal field acquires a strong dependence on the pump phase ϕ according to the relation (see SI)

$$G_j(\phi) = \frac{1}{1-\mu^2}\sqrt{1+\mu^2\eta^2 - 2\mu\eta\cos\phi} \qquad (3)$$

where $\mu = X_S/X_{S,th}$ is the pump amplitude normalized to the threshold amplitude for parametric instability, and $\eta = (\chi_j/\chi_i)^{1/2} \times (\bar{x}_i/\bar{x}_j)$ where $\bar{x}_{i,j}$ are the amplitudes of the membrane modes in the absence of the pump. As can be seen, the parameter $G_j(\phi)$ depends on both the amplitude and phase of the input signal field. In this sense, Eq(3) can be regarded as the mechanical equivalent of phase-sensitive amplification observed in nondegenerate optical parametric amplifiers (see, for example [31]).

We demonstrate phase-sensitive amplification by simultaneously monitoring the amplitudes of the signal and idler fields in the presence of the pump field. For these measurements, the signal and idler modes were weakly actuated while keeping their phases fixed. The pump (substrate) was actuated to different amplitudes below threshold while its phase, relative to the signal and idler, was slowly changed. The phase dependent amplification of the signal mode for different values of the normalized pump amplitude μ and pump phase ϕ is shown in Fig. 3. For these data, the signal mode was actuated to an amplitude of $35 \times (k_B T/m\omega_j^2)^{1/2}$ while the idler mode was actuated to an amplitude of $400 \times (k_B T/m\omega_i^2)^{1/2}$. The data show excellent agreement with the above expression, with observed parametric deamplification exceeding 20 dB. The pump amplitudes extracted from fits to these data are in agreement with the independently measured amplitudes to within 5% (Fig. 3 (inset)).

We make use of this nondegenerate parametric amplifier to demonstrate thermomechanical two-mode noise squeezing. In the absence of any actuation, the signal and idler membrane modes are subject only to thermomechanical noise. In this situation, if the pump field is driven below threshold, the membrane modes become highly correlated, with the correlations being manifest as a squeezing of a composite quadrature formed from linear combinations of quadratures of the individual membrane modes. This is the thermomechanical analog of two-mode squeezing seen in optical parametric amplifiers [32].

To quantify the degree of two-mode squeezing, we construct cross-quadratures from the displacements of the membrane modes, according to the relations $x_{a,b} = (\alpha_i \pm \alpha_j)/\sqrt{2}, y_{a,b} = (\beta_i \pm \beta_j)/\sqrt{2}$ where $\{\alpha_i, \beta_i\}$ are the respective quadratures of the individual membrane modes normalized to thermomechanical amplitudes. Phase-space distributions of these quadratures, accumulated over typical durations of 300 s, are shown in Fig. 4. The phase space distributions, which are symmetric in the absence of down-conversion, acquire a large ellipticity for

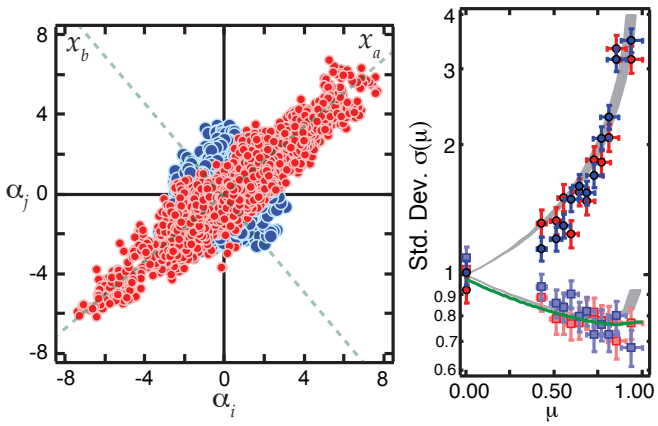

FIG. 4. Steady-state thermomechanical two-mode squeezing. Left: Phase space distributions of the quadratures α_i, α_j in the absence (blue) and presence (red) of the pump field, showing the emergence of correlations, i.e. noise squeezing, due to nondegenerate parametric amplification. Right: The standard deviations of the cross-quadratures x_a, y_b (red, blue), (amplified) and x_b, y_a (red, blue) (squeezed) *vs* pump amplitude. The shaded curves indicate the no-free-parameter prediction of our noise squeezing model based on independently measured parameters of our system. The green trace represents the expected degree of squeezing taking into account a finite measurement duration (see SI).

increasing amplitudes of the pump field. The data are in excellent agreement with our two-mode thermomechanical noise squeezing model (see Fig. 4 and SI). While an arbitrarily large degree of coherent deamplification may be obtained for specific relationships between the signal, idler and pump fields, our noise squeezing model predicts that the maximal degree of steady-state thermomechanical noise squeezing is limited by thermal averaging across all possible phases between the fields. Nonetheless, by harnessing feedback schemes based on weak measurements of the signal amplitude and phase, we estimate that mechanical squeezing of more than 40 dB may be obtained with our demonstrated parameters [19, 33, 34].

In summary, we realize strong, quantum-compatible multimode interactions in a macroscopic mechanical resonator through reservoir engineering, and use this nonlinear coupling to demonstrate nondegenerate parametric amplification and two-mode squeezing. This combination of strong nonlinear interactions, large $f \times Q$ products ($\gg k_B T/h$), low dissipation ($\gamma < (10\text{ s})^{-1}$) and compatibility with cavity optomechanical cooling and quantum-limited detection, provides a powerful tool for nonlinear approaches to quantum sensing and QND measurements of mechanical degrees of freedom. In addition, our work also paves the way towards the quantum manipulation of phononic fields for studies of macroscopic entanglement.

This work was supported by the DARPA QuASAR program through a grant from the ARO, an NSF INSPIRE award and the Cornell Center for Materials Re-

search with funding from the NSF MRSEC program (DMR-1120296). We acknowledge experimental assistance from A. Shaffer, H. F. H. Cheung and J. Geng. M. V. acknowledges support from the Alfred P. Sloan Foundation.

[1] T. J. Kippenberg and K. J. Vahala, Science **321**, 1172 (2008).
[2] M. Aspelmeyer, P. Meystre, and K. Schwab, Phys. Today **65**, 29 (2012).
[3] P. Meystre, Ann. der Phys. **525**, 215 (2013).
[4] M. Aspelmeyer, T. J. Kippenberg, and F. Marquardt, arXiv:1303.0733 (2013).
[5] J. D. Teufel, T. Donner, D. Li, J. W. Harlow, M. S. Allman, K. Cicak, A. J. Sirois, J. D. Whittaker, K. W. Lehnert, and R. W. Simmonds, Nature **475**, 359 (2011).
[6] J. Chan, T. P. Mayer Alegre, A. H. Safavi-Naeini, J. T. Hill, A. Krause, S. Gröblacher, M. Aspelmeyer, and O. Painter, Nature **478**, 89 (2011).
[7] J. D. Teufel, T. Donner, M. A. Castellanos-Beltran, J. W. Harlow, and K. W. Lehnert, Nature Nanotech. **4**, 820 (2009).
[8] G. Anetsberger, E. Gavartin, O. Arcizet, Q. P. Unterreithmeier, E. M. Weig, M. L. Gorodetsky, J. P. Kotthaus, and T. J. Kippenberg, Phys. Rev. A **82**, 061804(R) (2010).
[9] D. Rugar and P. Grütter, Phys. Rev. Lett. **67**, 699 (1991).
[10] V. Natarajan, F. DiFilippo, and D. E. Pritchard, Phys. Rev. Lett. **74**, 2855 (1995).
[11] R. B. Karabalin, R. Lifshitz, M. C. Cross, M. H. Matheny, S. C. Masmanidis, and M. L. Roukes, Phys. Rev. Lett. **106**, 094102 (2011).
[12] T. Faust, J. Rieger, M. J. Seitner, J. P. Kotthaus, and E. M. Weig, Nature Phys. **9**, 485 (2013).
[13] I. Mahboob, H. Okamoto, K. Onomitsu, and H. Yamaguchi, Phys. Rev. Lett. **113**, 167203 (2014).
[14] H. Seok, L. F. Buchmann, S. Singh, and P. Meystre, Phys. Rev. A **86**, 063829 (2012).
[15] A. D. O'Connell, M. Hofheinz, M. Ansmann, R. C. Bialczak, M. Lenander, E. Lucero, M. Neeley, D. Sank, H. Wang, M. Weides, J. Wenner, J. M. Martinis, and A. N. Cleland, Nature **464**, 697 (2010).
[16] J. Suh, M. D. LaHaye, P. M. Echternach, K. C. Schwab, and M. L. Roukes, Nano Lett. **10**, 3990 (2010).
[17] J. B. Hertzberg, T. Rocheleau, T. Ndukum, M. Savva, A. A. Clerk, and K. C. Schwab, Nature Phys. **6**, 213 (2010).
[18] J. Suh, A. J. Weinstein, C. U. Lei, E. E. Wollman, S. K. Steinke, P. Meystre, A. A. Clerk, and K. C. Schwab, Science **344**, 1262 (2014).
[19] A. Szorkovszky, G. A. Brawley, A. C. Doherty, and W. P. Bowen, Phys. Rev. Lett. **110**, 184301 (2013).
[20] A. Vinante and P. Falferi, Phys. Rev. Lett. **111**, 207203 (2013).
[21] A. Szorkovszky, A. A. Clerk, A. C. Doherty, and W. P. Bowen, New J. Phys. **16**, 043023 (2014).
[22] A. Pontin, M. Bonaldi, A. Borrielli, F. S. Cataliotti, F. Marino, G. A. Prodi, E. Serra, and F. Marin, Phys. Rev. A **89**, 023848 (2014).
[23] S. Diehl, A. Micheli, A. Kantian, B. Kraus, H. P. Büchler, and P. Zoller, Nature Phys. **4**, 878 (2008).
[24] A. Tomadin, S. Diehl, M. D. Lukin, P. Rabl, and P. Zoller, Phys. Rev. A **86**, 033821 (2012).
[25] H. Tan, G. Li, and P. Meystre, Phys. Rev. A **87**, 033829 (2013).
[26] Y. Wang and A. A. Clerk, Phys. Rev. Lett. **110**, 253601 (2013).
[27] S. Chakram, Y. S. Patil, L. Chang, and M. Vengalattore, Phys. Rev. Lett. **112**, 127201 (2014).
[28] T. P. Purdy, P. L. Yu, N. S. Kampel, R. W. Peterson, K. Cicak, R. W. Simmonds, and C. A. Regal, arXiv:1406.7247 (2014).
[29] D. Lee, M. Underwood, D. Mason, A. B. Shkarin, K. Borkje, S. M. Girvin, and J. G. E. Harris, arXiv:1406.7254 (2014).
[30] E. Gavartin, P. Verlot, and T. J. Kippenberg, Nat. Commun. **4:2860** (2013).
[31] R. Tang, J. Lasri, P. S. Devgan, V. Grigoryan, and P. Kumar, Opt. Exp. **13**, 10483 (2005).
[32] M. D. Reid and P. D. Drummond, Phys. Rev. Lett. **60**, 2731 (1988).
[33] G. Björk and Y. Yamamoto, Phys. Rev. A **37**, 125 (1988).
[34] A. A. Clerk, F. Marquardt, and K. Jacobs, New J. Phys. **10**, 095010 (2008).